ACADÉMIE
DES SCIENCES
INSTITUT DE FRANCE

Comptes Rendus
Mécanique

Brahim Bouaziz, Maher Eltaief and Chokri Bouraoui

An engineering methodology for predicting crack growth of 2024-T3 aluminium alloys under variable amplitude loading

Volume 353 (2025), p. 1385-1404

Online since: 9 December 2025

https://doi.org/10.5802/crmeca.339

The Comptes Rendus. Mécanique *are a member of the Mersenne Center for open scientific publishing*
www.centre-mersenne.org — e-ISSN : 1873-7234

ACADÉMIE DES SCIENCES
INSTITUT DE FRANCE

Comptes Rendus. Mécanique
2025, Vol. 353, p. 1385-1404
https://doi.org/10.5802/crmeca.339

Research article

An engineering methodology for predicting crack growth of 2024-T3 aluminium alloys under variable amplitude loading

Brahim Bouaziz [*,a], **Maher Eltaief** [a] **and Chokri Bouraoui** [a]

[a] Mechanical Laboratory of Sousse, National Engineering School of Sousse, University of Sousse, BP 264, Erriadh, 4023 Sousse, Tunisia

E-mails: bouaziz_ibrahim@yahoo.fr (B. Bouaziz), eltaiefmaher@gmail.com (M. Eltaief), chokri.bouraoui2@gmail.com (C. Bouraoui)

Abstract. The propagation of fatigue cracks can significantly reduce the lifespan of components, potentially leading to failures. This study presents an engineering approach that accounts for variable-amplitude loading while incorporating residual stresses at the crack tip.

The objective is to evaluate the fatigue life of 2024-T3 aluminum alloys under variable loading by transforming the problem into an equivalent one with constant loading, eliminating complex cycle-by-cycle calculations.

The proposed strategy is integrated into the two-parameter fatigue crack growth model, which considers both the total maximum stress intensity factor K_{max_tot} and the total stress intensity factor range ΔK_{tot}. Initially, plastic zone interaction effects are neglected to establish an equivalence relationship between variable and constant loading.

The Willenborg model is then used to determine the equivalent stress, ensuring a comparable crack growth rate. To refine the approach, a finite element (FE) elasto-plastic analysis based on the Chaboche model is conducted. This analysis estimates the residual stress distribution at the crack tip, converted into a residual stress intensity factor K_r. This factor is integrated into a correction coefficient equation to account for plastic zone interaction effects.

Three loading spectra were examined. Predicted results were compared with experimental data, showing that the proposed model improves crack growth life in 2024-T3 aluminum alloy structures subjected to variable-amplitude loading.

Keywords. Fatigue crack growth life, Variable amplitude loading, Residual stress intensity factor, Equivalent stress level, Optimization.

Manuscript received 2 July 2025, revised 27 September 2025 and 29 October 2025, accepted 31 October 2025.

1. Introduction

In most structural components used in the automotive or aerospace industries, the presence of cracks or geometric discontinuities is inevitable. These components are often subjected to cyclic loading of variable amplitude. To reduce the risk of failure, fatigue life prediction is a fundamental step in the design process. Considering both the importance of safety and the current economic context in this sector, research on extending the service life of these structures remains highly relevant. Throughout their service life, structures are subjected to random loads, which makes estimating crack growth and consequently, fatigue life difficult and unreliable. Fatigue crack growth (FCG) is influenced not only by the current load but also by the loading

* Corresponding author

history [1–3], which induces interaction effects in the plastic zone, either accelerating or slowing down crack propagation under realistic service conditions, sequence effects arising from the order and magnitude of load surges and relaxations can modify the local plastic zone and induce memory in the material, thereby altering crack growth paths in ways that simple ΔK criteria cannot capture. Numerous studies have been carried out in recent decades to predict fatigue crack growth under variable loading. Some of these have focused on calculating the size of the plastic zone and its effect on propagation delay, as first proposed by Wheeler [3–5]. Others focus on the concept of crack closure and its impact on propagation behaviour, where Elber [6,7] was the first to introduce this concept. Later, Noorozi and Glinka [8] proposed a two-parameter model for the analysis of fatigue crack growth, based on the elastic–plastic response ahead of the crack tip. The prediction of fatigue life under the effect of a variable load is a major issue for components and structures working under real service conditions. This study aims to develop an engineering methodology that accounts for various types of variable-amplitude loading, considering residual stresses at the crack tip. In this context, the objective is to estimate fatigue life under variable loading by replacing it with an equivalent problem where the loading is constant, which is easier to handle, while taking into account the effects of random loading sequences [9]. In this paper, an equivalent stress transformation approach is substituted for the two-parameter fatigue crack growth model. This choice is physically justified: plastic interactions and residual stresses generated at the crack tip modulate the load gradients and, consequently, the driving force that governs propagation. Firstly, all plasticised zone interaction effects are neglected, allowing an equivalence relationship to be established between variable loads and constant loading using the driving force model [8,10], which states that fatigue crack growth behaviour combines both the total maximum stress intensity factor $K_{\max\_tot}$ and the magnitude of the total stress intensity factor ΔK_{tot}. Secondly, the Willenborg model [11], generalised by Meggiolaro and Castro [12,13] and Gallagher [13,14], is used to determine the equivalent stress $\Delta\sigma_{eq}$ deduced from variable loading, which causes a similar level of crack growth to that caused by constant loading. However, the limitations of the Willenborg model [11] in particular its inability to account for the influence of multiple overloads and under loads and, therefore, to predict a lifetime greater than that determined without the plastic–zone interaction [15] effect justify the use of finite element (FE) analysis to incorporate the effect of this zone. This makes it possible to consider the effect of residual stresses induced by plastic deformation at the bottom of the crack on the lifetime prediction. In this study, we propose an innovative association between the driving force model and the Willenborg model [11], complemented by FE integration, to predict the fatigue crack growth of structural components subjected to real loads. The present work is organised as follows:

(i) Determination of equivalent loads at constant amplitudes without accounting plastic deformation into account.
(ii) Determination of driving force modulus parameters from experimental data.
(iii) FE modelling of residual stresses induced by plastic deformation at the bottom of the crack.
(iv) Determination of corrected equivalent loads at constant amplitudes, taking plastic deformation into account.

2. Procedure for calculating equivalent stresses

2.1. *Equivalent stress without crack closure effect*

Throughout its service life, each structural component undergoes actual loading in the form of load spectra with varying magnitudes and stress ratios. The objective, described in

references [16,17], is to find a relationship that describes crack growth by applying a constant load similar to that of the variable loads. This work modifies this approach by using the finite element tool to take into account the interactions of plastic zones and the effect of residual stresses on crack growth prediction. A correction coefficient is implemented, depending on the parameters of the driving force model, the maximum stress intensity factor and the residual stress intensity factor, in order to adjust the calculated equivalent stress without taking into account the effect of plastic zone interaction.

The two-parameter driving force model is used to estimate fatigue crack growth, incorporating both the total maximum stress intensity factor $K_{\max,\text{tot}}$ and the total stress intensity factor range ΔK_{tot}. The equation below describes the crack growth rate:

$$\frac{\mathrm{d}a}{\mathrm{d}N} = CK_{\max}^{p}\Delta K^{q}, \tag{1}$$

where C, p, q are the calibration parameters of the fatigue crack growth data.

In the case of linear damage, and when a crack is subjected to a cyclic load spectrum of variable amplitude such as $\Delta\sigma_i$ for N_i cycles, the crack length during this spectrum is Δa which can be calculated from crack growth rates such as [18]:

$$\Delta a = \left(\frac{\mathrm{d}a}{\mathrm{d}N}\right)_1 \cdot N_1 + \left(\frac{\mathrm{d}a}{\mathrm{d}N}\right)_2 \cdot N_2 + \cdots + \left(\frac{\mathrm{d}a}{\mathrm{d}N}\right)_n \cdot N_n. \tag{2}$$

From the formulation in Equation (1), Equation (2) can be rewritten as follows

$$\Delta a = C(K_{1\max}^{p}\Delta K_1^{q}N_1 + K_{2\max}^{p}\Delta K_2^{q}N_2 + \cdots + K_{n\max}^{p}\Delta K_n^{q}N_n). \tag{3}$$

Since the crack closure effect is negligible, the relationship between the maximum stress intensity factor $K_{\max}$ and the stress intensity factor range ΔK is given by [18]:

$$K_{\max} = \frac{\Delta K}{1-R}, \tag{4}$$

where R is the stress ratio, defined as $\sigma_{\min}/\sigma_{\max}$.

We can rewrite the expression for crack length as a function of ΔK as follows:

$$\begin{aligned}\Delta a &= C\left(\left(\frac{\Delta K_1}{1-R_1}\right)^{p}\Delta K_1^{q}N_1 + \left(\frac{\Delta K_2}{1-R_2}\right)^{p}\Delta K_2^{q}N_2 + \cdots + \left(\frac{\Delta K_n}{1-R_n}\right)^{p}\Delta K_n^{q}N_n\right)\\ &= C\left(\frac{\Delta K_1^{p+q}}{(1-R_1)^{p}}N_1 + \frac{\Delta K_2^{p+q}}{(1-R_2)^{p}}N_2 + \cdots + \frac{\Delta K_n^{p+q}}{(1-R_n)^{p}}N_n\right).\end{aligned} \tag{5}$$

The range of stress intensity factors ΔK is expressed as a function of stress level and crack length:

$$\Delta K = Y\Delta\sigma\sqrt{\pi a}, \tag{6}$$

where Y represents a geometric correction factor.

Thus, the total crack length can be rewritten as:

$$\Delta a = C\cdot Y^{p+q}(\pi a)^{(p+q)/2}\cdot\left(\frac{\Delta\sigma_1^{p+q}}{(1-R_1)^{p}}N_1 + \frac{\Delta\sigma_2^{p+q}}{(1-R_2)^{p}}N_2 + \cdots + \frac{\Delta\sigma_n^{p+q}}{(1-R_n)^{p}}N_n\right). \tag{7}$$

From Equation (7), it is possible to calculate the growth of the equivalent crack from a constant amplitude loading:

$$\Delta a = C\cdot Y^{p+q}(\pi a)^{(p+q)/2}\cdot\left(\frac{\Delta\sigma_{\text{eq}}^{p+q}}{(1-R_{\text{eq}})^{p}}N_{\text{total}}\right). \tag{8}$$

Equality between Equations (7) and (8) allows us to calculate $\Delta\sigma_{\text{eq}}$:

$$\Delta\sigma_{\text{eq}} = \left(\sum_{i=1}^{n}\frac{N_i}{N_{\text{total}}}\frac{(1-R_{\text{eq}})^{p}}{(1-R_i)^{p}}\Delta\sigma_i^{p+q}\right)^{1/(p+q)}. \tag{9}$$

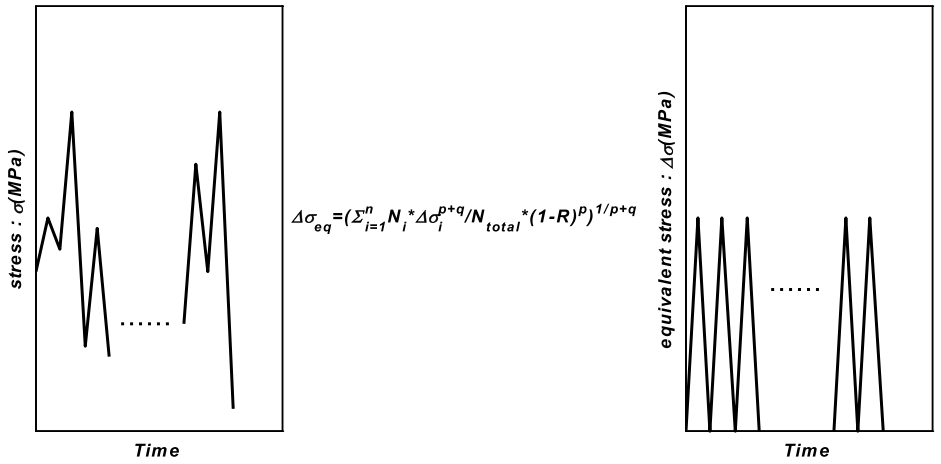

Figure 1. Equivalent stress.

Since the equivalent constant load is assumed to vary between 0 and $\sigma_{\max}$, hence $R_{\text{eq}} = 0$, the equivalent stress is given by:

$$\Delta\sigma_{\text{eq}} = \left(\sum_{i=1}^{n} \frac{N_i}{N_{\text{total}}} \frac{\Delta\sigma_i^{p+q}}{(1-R_i)^p}\right)^{1/(p+q)}. \tag{10}$$

By combining the two-parameter model with the Willenborg model, the crack growth rate can be described in this form [19]:

$$\frac{\mathrm{d}a}{\mathrm{d}N} = CK_{\max}^{p}\Delta K_{\text{eff}}^{q} = \frac{C}{(1-R)^p}\Delta K_{\text{eff}}^{p+q} = C_T\Delta K_{\text{eff}}^{p+q}, \tag{11}$$

where R is the stress ratio for constant loading. Several studies carried out on aluminium alloys show that $p = 2$ [20,21]. In Equation (11), it can be seen that there are two unknowns to be determined: the coefficient C_T and q, which will be deduced from experimental data on the crack growth rate curve ($\mathrm{d}a/\mathrm{d}N$) as a function of ΔK under constant load (R = constante).

The Willenberg model [11] used predicts a maximum delay just after the overload, which does not allow the influence of multiple overloads and under loads to be predicted correctly, as the lifetime is on average equivalent to that determined without the effect of plastic zone interaction [15].

Figure 1 illustrates the procedure for converting a variable load into an equivalent constant load at $R = 0$.

2.2. *Effect of crack closure on equivalent stress*

In this section, the two-parameter driving force model is modified to account for the effect of crack closure on crack propagation [8].

Residual stresses play a crucial role in crack growth prediction. To integrate them into the driving force model, weight functions are used to convert the residual stress distribution into a residual stress intensity factor K_{r} [22], which is added only to the maximum stress intensity factor since residual stresses do not influence the minimum stress intensity factor [23]. The range of total stress intensity factors and the total maximum stress intensity factor can be defined as follows [24]:

$$\begin{cases} K_{\max\_\text{tot}} = K_{\max\_\text{app}} + K_{\text{r}} \\ \Delta K_{\text{tot}} = \Delta K_{\text{app}}. \end{cases} \tag{12}$$

The crack growth rate, as indicated in Equation (1), is modified:

$$\left(\frac{\mathrm{d}a}{\mathrm{d}N}\right)_{\text{corrected}} = C(K_{\max} + K_{\mathrm{r}})^{p}(\Delta K_{\text{app}})^{q}. \tag{13}$$

The link between Equations (13) and (1) allows us to define a coefficient such that:

$$\frac{\left(\frac{\mathrm{d}a}{\mathrm{d}N}\right)_{\text{corrected}}}{\frac{\mathrm{d}a}{\mathrm{d}N}} = \frac{(K_{\max} + K_{\mathrm{r}})^{p}(\Delta K_{\text{app}})^{q}}{K_{\max}^{p}\Delta K_{\text{app}}^{q}} = \left(\frac{K_{\max} + K_{\mathrm{r}}}{K_{\max}}\right)^{p} = \left(1 + \frac{K_{\mathrm{r}}}{K_{\max}}\right)^{p}. \tag{14}$$

Thus, the effect of crack closure is deduced by a correction coefficient that depends on the stress intensity factor at each cycle, the residual stress intensity factor and the material coefficients p and q.

The corrected crack growth rate is given by:

$$\left(\frac{\mathrm{d}a}{\mathrm{d}N}\right)_{\text{corrected}} = \left(1 + \frac{K_{\mathrm{r}}}{K_{\max}}\right)^{p}\frac{\mathrm{d}a}{\mathrm{d}N}. \tag{15}$$

Referring to Equations (4) and (6), the crack growth rate is expressed as follows:

$$\frac{\mathrm{d}a}{\mathrm{d}N} = CK_{\max}^{p}\Delta K^{q} = C\frac{\Delta K^{p+q}}{(1-R)^{p}} = \frac{C}{(1-R)^{p}}(Y\Delta\sigma_{\text{eq}}\sqrt{\pi a})^{p+q}. \tag{16}$$

By combining Equations (15) and (16), the corrected crack growth rate is expressed as follows:

$$\begin{aligned}\left(\frac{\mathrm{d}a}{\mathrm{d}N}\right)_{\text{corrected}} &= \frac{C}{(1-R)^{p}}(Y\Delta\sigma_{\text{eq\_corrected}}\sqrt{\pi a})^{p+q} \\ &= \left(1 + \frac{K_{\mathrm{r}}}{K_{\max}}\right)^{p}\frac{C}{(1-R)^{p}}(Y\Delta\sigma_{\text{eq}}\sqrt{\pi a})^{p+q}.\end{aligned} \tag{17}$$

Incorporating the residual stresses generated by plastic deformation, the corrected equivalent stress is determined from the earlier equivalent-stress expression in Equation (10):

$$\Delta\sigma_{\text{eq\_corrected}} = \left(1 + \frac{K_{\mathrm{r}}}{K_{\max}}\right)^{\frac{p}{p+q}}\Delta\sigma_{\text{eq}} = \mu\Delta\sigma_{\text{eq}}, \tag{18}$$

where μ is defined as:

$$\mu = \left(1 + \frac{K_{\mathrm{r}}}{K_{\max}}\right)^{\frac{p}{p+q}}. \tag{19}$$

A correction is then made to $\Delta\sigma_{\text{eq}}$ found in Equation (10), corresponding to equivalent amplitude loading at $R = 0$, as illustrated in the Figure 2.

3. Procedure for calculating correction coefficient μ

This coefficient is used to introduce the effect of plastic zone interactions on the equivalent constant stress level and it depends on the properties of the material, the maximum stress intensity factor and the residual stress intensity factor. The transition from an equivalent constant stress level in Equation (10) to a corrected equivalent stress level in Equation (18) is adjusted by this coefficient in Equation (19).

This coefficient is computed cycle by cycle, allowing for an accurate estimation of its impact on service fatigue life.

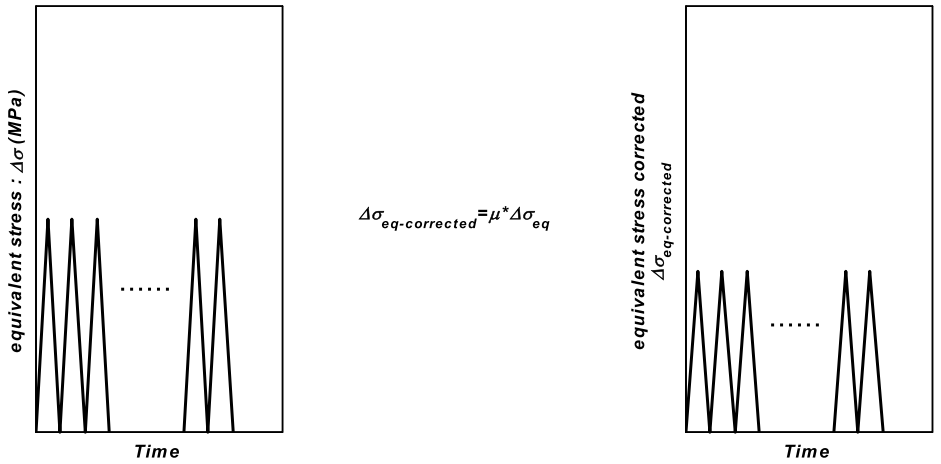

Figure 2. Corrected equivalent load.

3.1. *Calculation of the equivalent residual stress intensity factor* K_{r}

To estimate the equivalent residual stress distribution σ_{r} created upstream of the crack tip, the FE method is used. At the end of unloading, the residual stress distribution is extracted, which will remain constant during constant amplitude loading. A simulation on ABAQUS [25], close to the crack tip, was carried out, where the behaviour close to the crack tip is based on the Chaboche model [26]. This model is capable of describing the cyclic response of plastic deformation upstream of the crack under constant and variable loading. Elasto-plastic finite element analysis is used to determine the residual stress distribution σ_{r} ahead of the crack tip under constant cyclic loading of maximum value $\Delta\sigma_{\mathrm{eq}}$ and load ratio $R = 0$. Then, the residual stress intensity factor K_{r} is deduced using the following relationship [22]:

$$K_{\mathrm{r}} = \int \sigma_{\mathrm{r}} m(x,a)\,\mathrm{d}x, \tag{20}$$

where x represents the position of the point along the crack front and $m(x,a)$ is the weight function, given by [27]:

$$m(x,a) = \frac{2P}{\sqrt{2\pi(a-x)}}, \tag{21}$$

where P represents the load applied.

3.2. *Calculation of the maximum stress intensity factor* $K_{\max}$

The prediction of crack increment evolution is influenced at each loading cycle by various parameters including material properties, loading type, specimen geometry, location and initial crack size a_0. Each variation in these parameters leads to the evolution of the crack, controlled by the stress intensity range and the maximum stress intensity factor. Indeed, for loading "i", the maximum stress intensity factor is expressed as follows:

$$K_{\max,i} = Y\Delta\sigma_{\mathrm{eq}}\sqrt{\pi a_i}, \tag{22}$$

where Y is the geometric factor that depends on both the geometry considered and the loading mode. The value of Y can be estimated either through extensive stress analyses using finite element methods or by employing available ready-made solutions [28].

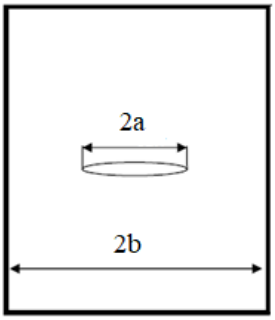

Figure 3. Example of middle-tension specimen.

The most well-known and used Y factor solutions for middle-tension Figure 3 specimens under tension loading are:

$$Y = \frac{1 - 0 \cdot 5\left(\frac{a}{b}\right) + 0 \cdot 32\left(\frac{a}{b}\right)^2}{\sqrt{1 - \frac{a}{b}}}, \tag{23}$$

where a is a crack length and b is a specimen width.

3.3. *Calculation of calibration parameters C_T, p, q*

To establish these parameters, we utilize experimental data for the crack growth rate curve ($\mathrm{d}a/\mathrm{d}N$) in relation to the range of the stress intensity factor (ΔK) under a constant load. The curve depicting the relation ship between the crack growth rate ($\mathrm{d}a/\mathrm{d}N$) and the (ΔK) range is employed to fine-tune the parameters p, q, and C_T. Multiple studies on aluminum alloys (Al-2024-T3) have shown that $p = 2$ [20,21], this fixed exponent serves as a reference for calibrating additional coefficients C_T and q. These parameters are then incorporated into the equation for calculating the equivalent load.

3.4. *Optimisation of the correction coefficient μ*

From Equation (22), for the maximum stress intensity factor for each cycle, one observes that the maximum stress intensity factor varies from cycle to cycle, which drives a variation in the correction coefficient μ that is also variable. The aim is to have, in a practical framework, a correction coefficient μ that enables mapping a variable real load to a stabilized equivalent stress, thereby facilitating life estimation.

According to Equation (19), the correction factor is introduced as:

$$\mu_i = \left(1 + \frac{K_{\mathrm{r}}}{K_{\max,i}}\right)^{\frac{p}{p+q}} \tag{24}$$

which implies that the correction coefficient μ depends on the material properties p and q, on the maximum stress intensity factor $K_{\max,i}$ for each cycle and on the residual stress intensity factor K_{r}. In practice, the variation of $K_{\max,i}$ from cycle to cycle induces a variation in the correction coefficient μ_i.

In typical load sequences (e.g., recurrent spectra or block loading), variations in correction coefficient μ can be considered by its average value of the cycle mean and the distribution of cycles do not dramatically alter the distribution of $K_{\max,i}$. In this context, fixing the correction coefficient μ to a representative mean value computed from a representative set of cycles can

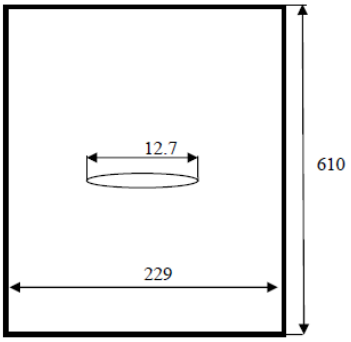

Figure 4. Specimen dimension.

provide an effective estimate of the corrected equivalent stress without requiring continuous recalibration. But if the load sequence varies strongly (e.g., frequent alternating peaks and troughs, or abrupt transitions between loading regimes), the correction coefficient μ may become sensitive to the sequence and require periodic recalibration.

In this study, the approach adopted initially is to use a constant value of the correction coefficient μ to simplify the estimation of the corrected equivalent stress defined by Equation (18): $\Delta\sigma_{\text{eq\_corrected}} = \mu\Delta\sigma_{\text{eq}}$, where $\Delta\sigma_{\text{eq}} = f(\Delta\sigma)$, Equation (10), as described previously in the model framework, with $\Delta\sigma$ representing the actual variable load and $\Delta\sigma_{\text{eq}}$ the constant equivalent load.

According to Equation (22), the distribution of $K_{\max,i}$ is not strongly affected by the cycle distribution, as $\Delta\sigma_{\text{eq}}$ remains constant, therefore, the correction coefficient μ may vary modestly around a mean value. Fixing the correction coefficient μ to a representative mean can thus provide an effective estimate of the corrected equivalent stress.

4. Numerical application

4.1. *A plate with a central crack*

The analysis was carried out on a sample (Figure 4) of 2024-T3 aluminium alloy with a central crack of initial size ($2a$) equal to 12.7 mm, a length L of 610 mm, a width w of 229 mm and a thickness t of 4.1 mm.

4.2. *Calculation of parameters C_T, q*

To determine the equivalent load according to Equation (10), it is necessary to find the unknown q (the value of p being equal to 2). This is done using Equation (11), which has two unknowns (C_T and q). In order to determine these two parameters, experimental data of the crack growth rate curve $\mathrm{d}a/\mathrm{d}N$ as a function of the stress intensity factor range ΔK under constant load is used. Then, the following curve (Figure 5) represents the variation of the crack growth rate $\mathrm{d}a/\mathrm{d}N$ as a function of the stress intensity range ΔK is used to fit the parameters p, q and C_T.

For an aluminium alloy, we take $p = 2$, which makes it possible to determine $C_T = 1.2037 \times 10^{-11}$ and $q = 1.7877$.

4.3. *Calculation of the equivalent stress $\Delta\sigma_{\text{eq}}$*

We then use the loading block shown in Figure 6, according to references [30].

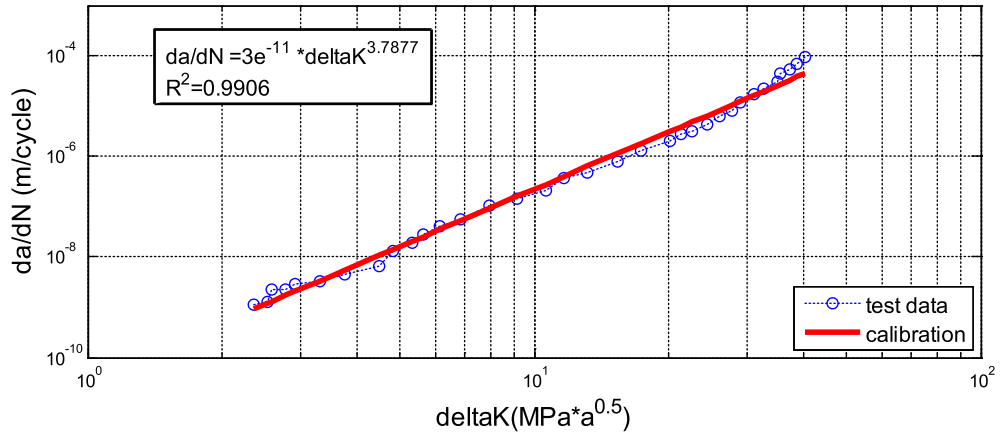

Figure 5. $(\mathrm{d}a/\mathrm{d}N) - \Delta K$ of 2024-T3 aluminium alloys for $R = 0.4$ [29].

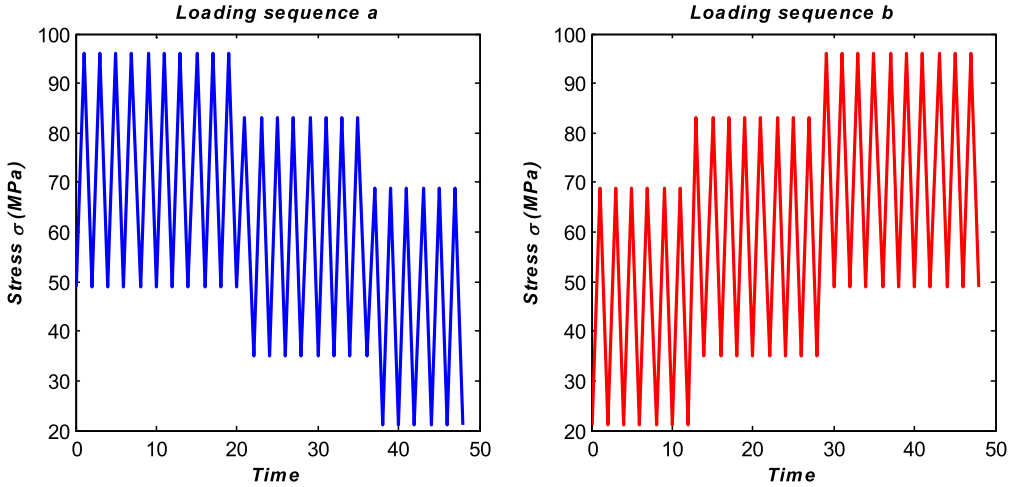

Figure 6. Loading sequence.

According to Equation (10), the equivalent load associated with each loading sequence is expressed in the following form:

$$\Delta\sigma_{\mathrm{eq}} = \left(\sum_{i=1}^{3} \frac{N_i}{N_{\mathrm{total}}} \frac{\Delta\sigma_i^{p+q}}{(1-R_i)^p} \right)^{1/(p+q)}, \tag{25}$$

where the load ratio $R = 0$ leads to $\Delta\sigma_{\mathrm{eq}} = \sigma_{\max}$.

4.4. *Calculation of the residual stresses* σ_{r}

The residual stress generated ahead the crack tip, extracted at the end of unloading phase, are estimated using FE analysis based on the Chaboche model [26], this model can describe cyclic plasticity with high precision by accounting for the Bauschinger effect, mean stress relaxation, and cyclic hardening during simulations. In our study, the nonlinear kinematic hardening model is integrated into ABAQUS to evaluate the influence of a variable-amplitude loading on the cyclic plastic behavior at the crack tip of the 2024-T3 aluminum alloy.

Table 1. Summary of cyclic fatigue and mechanical properties of Al2024-T3 alloy [31]

E (MPa)	ν	σ_y (MPa)	C_1 (MPa)	C_2 (MPa)	C_3 (MPa)	γ_1	γ_2	γ_3
73 000	0.33	289	2169.7	7471.9	65.761	11.74	90.05	555.09

E is the elastic modulus, ν is the Poisson's ratio, σ_y is the yield stress, C_1, C_2 and C_3 are the kinematic stress parameter for the back stress and γ_1, γ_2 and γ_3 are the corresponding kinematic saturation rate parameter.

The Von Mises criterion applied in this study is defined by the following expression:

$$f(\overline{\overline{\sigma}}, \overline{\overline{X}}) = J_2(\overline{\overline{\sigma}} - \overline{\overline{X}}) - \sigma_y, \tag{26}$$

where f is the elasticity surface, $J_2(\overline{\overline{\sigma}} - \overline{\overline{X}})$ indicates the second invariant of the stress deviator tensor and σ_y is the elastic limit.

The non-linear hardening component $\overline{\overline{X}}$ is described by the following equation:

$$\mathrm{d}\overline{\overline{X}} = \tfrac{2}{3} C_i \dot{\overline{\overline{\varepsilon}}}^{p} - \gamma_i \overline{\overline{X}} p^{\cdot}, \tag{27}$$

where $\dot{\overline{\overline{\varepsilon}}}^{p}$ is the plastic strain tensor and $p^{\cdot}$ the cumulative plastic deformation rate, which are defined as follows:

$$p^{\cdot} = \sqrt{\frac{2}{3} \dot{\overline{\overline{\varepsilon}}}^{p} : \dot{\overline{\overline{\varepsilon}}}^{p}} \tag{28}$$

$$\dot{\overline{\overline{\varepsilon}}}^{p} = \underline{\lambda} \frac{\delta f}{\delta \sigma}. \tag{29}$$

In order to correctly predict the kinematic effect, several parameters are introduced, in which C_i and γ_i represent the characteristic parameters of each material.

This residual stress distribution remains unchanged under constant amplitude loading. The mechanical and cyclic fatigue properties of the Al2024-T3 alloy are summarised in the Table 1, where C_i and γ_i represent the Chaboche kinematic hardening parameters.

Figures 7 and 8 illustrate the finite element model, as well as the boundary conditions and the type of mesh used.

To enhance result accuracy and better predict the crack tip response to plastic deformation in the FE analysis, a highly refined mesh was applied around the $CPS4R$ crack region, with an element size of 0.05 [3,24]. This FE analysis results in a residual stress distribution, as shown in Figure 9.

Using the FE method, the residual stress is estimated based on the S_{22} stress distribution. It is observed that the compressive stress distribution increases in absolute value near the crack tip, which is confirmed by the results of several researchers [32].

To take account of the effect of the loading sequence, the residual stresses are estimated from the loading sequences (a and b) shown in Figure 6 and then compared to the residual stresses determined from the equivalent load calculated from Equation (25).

Equations (20) and (21) are used to calculate the residual stress intensity factor K_{r}.

4.5. *Calculation of the maximum stress intensity factor* $K_{\max}$

The aim now is to estimate the correction coefficient μ and, subsequently, the value of the corrected equivalent stress from Equation (18).

The correction coefficient is given in Equation (24). In this equation; the coefficients p, q and K_{r} are constant, while the maximum stress intensity factor $K_{\max}$ is variable and depends on the crack length a according to Equation (22).

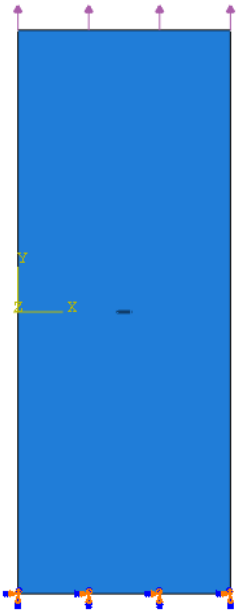

Figure 7. Boundary conditions used in the simulation.

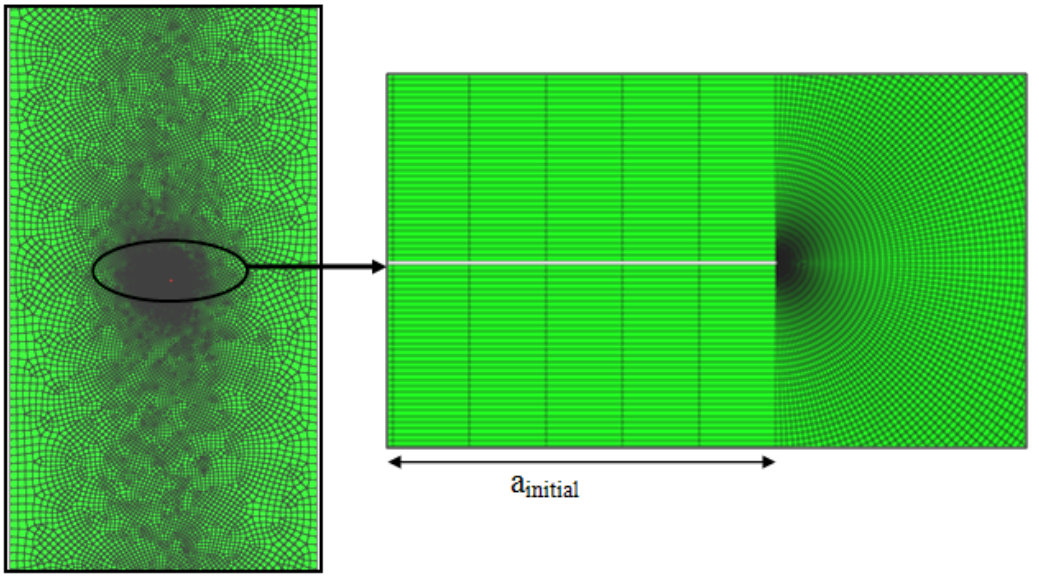

Figure 8. Type of finite element mesh.

The variation of $\Delta\sigma_{eq}$ is calculated from Equation (10). In this study, the applied load is $\Delta\sigma_{eq} = \sigma_{max} = 62,63$ MPa. The variation of μ as a function of K_{max} is shown in the following figure for the two loading sequences (a and b) illustrated in Figure 10 and is compared with that deduced from the equivalent load.

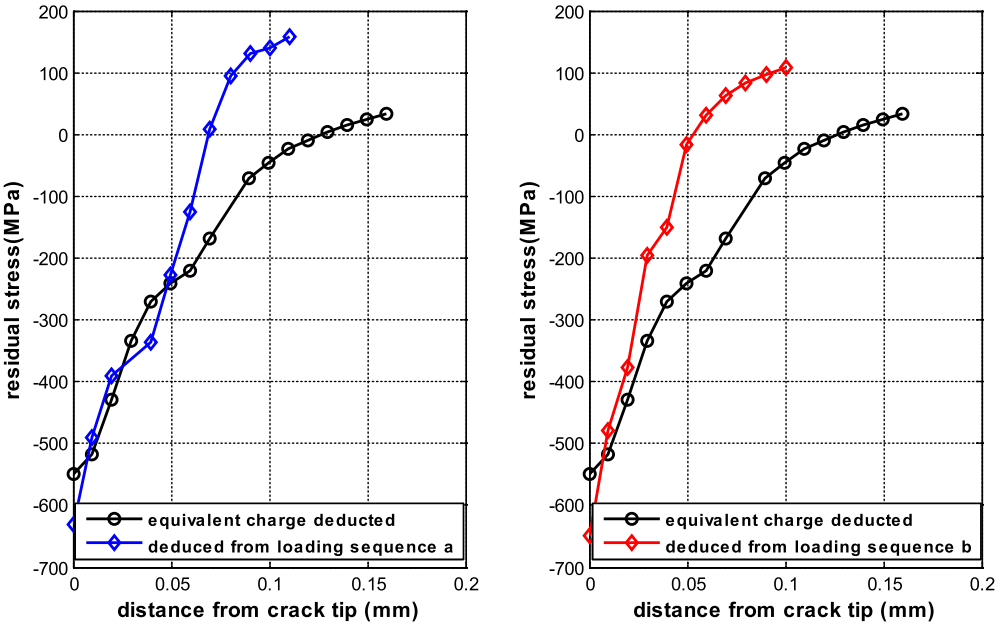

Figure 9. Stress distribution.

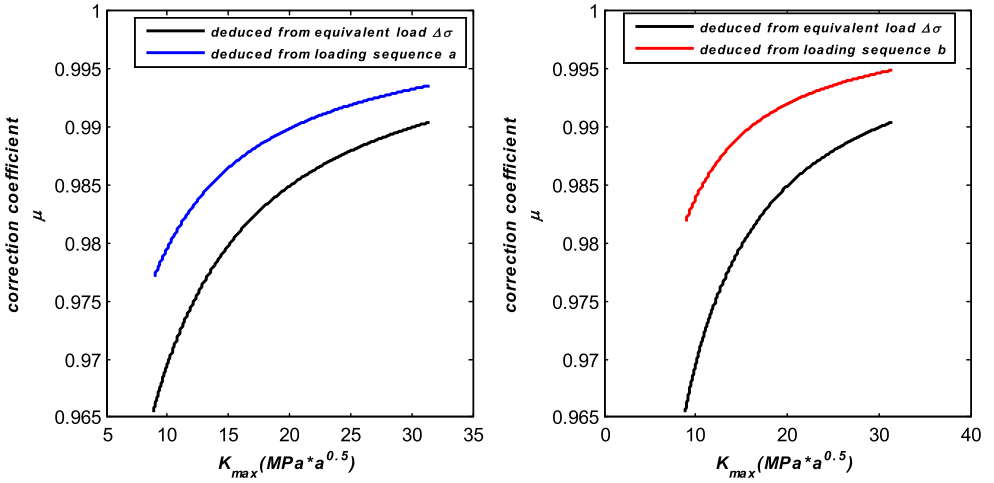

Figure 10. Variation of μ as a function of $K_{\max}$.

4.6. *Optimisation of the correction coefficient* μ

Combining Equation (18) with Equation (24), we obtain:

$$\Delta\sigma_{\text{eq\_corrected},i} = \mu_i \Delta\sigma_{\text{eq}}. \tag{30}$$

We therefore look for determining μ_i allowing us to obtain $\Delta\sigma_{\text{eq\_corrected},i}$ to predict a lifetime as close as possible to the experimental results. Table 2 shows some calculation points taken from the correction coefficient curve (Figure 11), where the residual stress is deduced from the equivalent load.

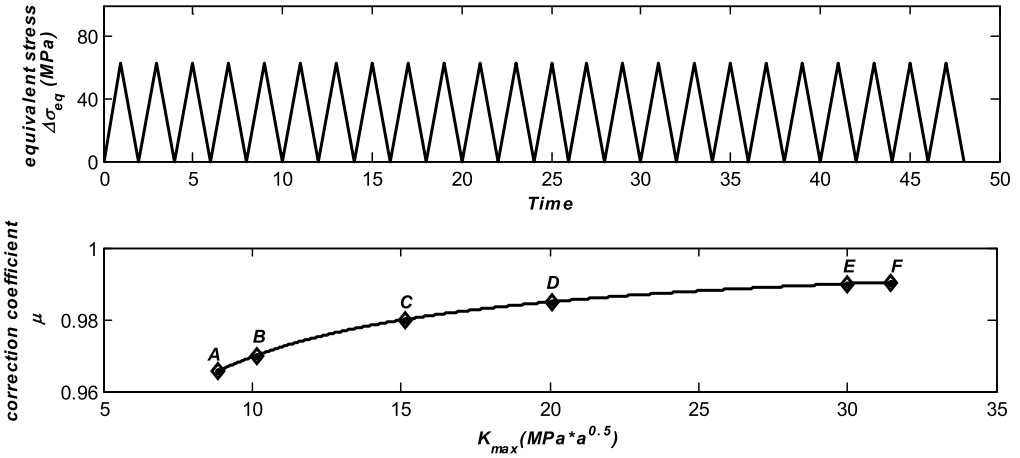

Figure 11. Variation of μ as a function of $K_{\max}$ (equivalent residual stress).

Table 2. Effect of correction coefficient μ on equivalent load

Point	μ	$\Delta\sigma_{\text{eq\_corrected}}$
A	0.9655	60.4776
B	0.97	60.7594
C	0.98	61.3858
D	0.985	61.699
E	0.99	62.0122
F	0.9904	62.0373

Figure 12 shows the effect of the correction coefficient on the variation curve of the crack length a (mm) as a function of the number of cycles N (cycles) for the two loading sequences (a and b).

The values of the correction coefficients obtained at different points will be multiplied by $\Delta\sigma_{\text{eq}}$ to determine $\Delta\sigma_{\text{eq\_corrected}}$. Thus, for each cyclic loading spectrum corresponds an equivalent loading $\Delta\sigma_{\text{eq}}$ multiplied by a selected correction coefficient μ_i, leading to the $\Delta\sigma_{\text{eq\_corrected}}$ corresponding to a curve dipicting the evolution crack length as a function of the number of cycles. It is observed that the lower this factor, the closer the curve is to the experimental results.

We can conclude that a minimal correction coefficient, corresponding to the first iteration ($i = 1$), where the maximum stress intensity $K_{\max}$ and crack length are minimal ($a = a_0$), is the optimal coefficient (corresponding to point A in Figure 11), as it offers a variation in crack length as a function of the number of cycles that is most consistent with the experimental curve.

To take account of the effect of the loading sequence, we consider the minimum values of the correction coefficients for each loading sequence (according to Figure 13) and compare them with the results from point A.

We obtain the results on the variation of the crack size as a function of the number of cycles for the selected points, as follows (Figure 14).

It can be seen that the correction coefficient corresponding to point A, where residual stresses are deduced from constant loads (equivalent load), produces a variation in crack size as a function of the number of cycles that is closest to the experimental results. In comparison, the curve produced by the coefficient corresponding to point A1, where the residual stresses are deduced from the variable loads (loading sequence a), differs, as does that produced by the

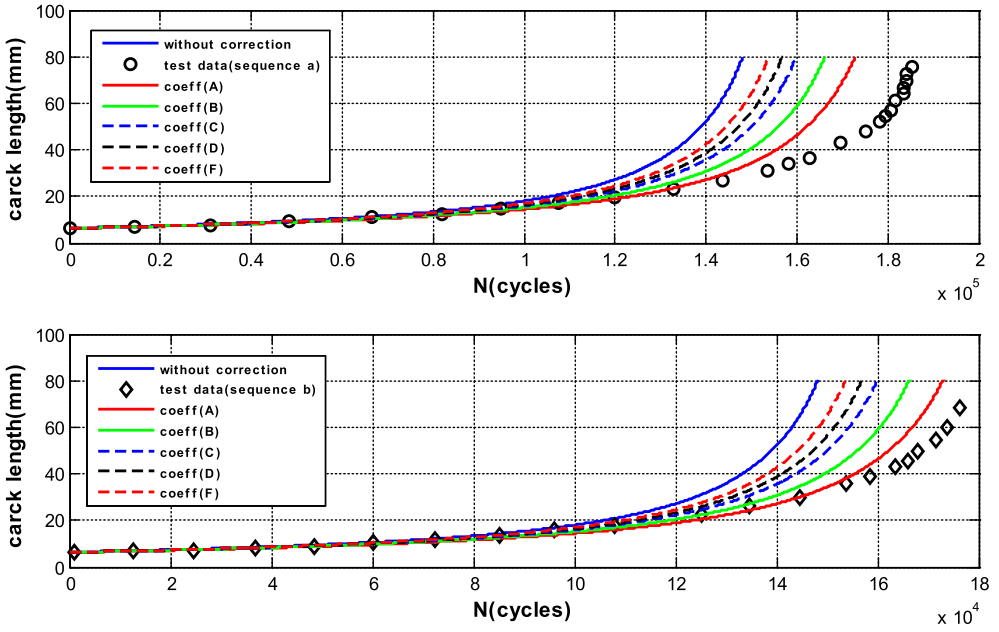

Figure 12. Effect of correction coefficient on crack evolution.

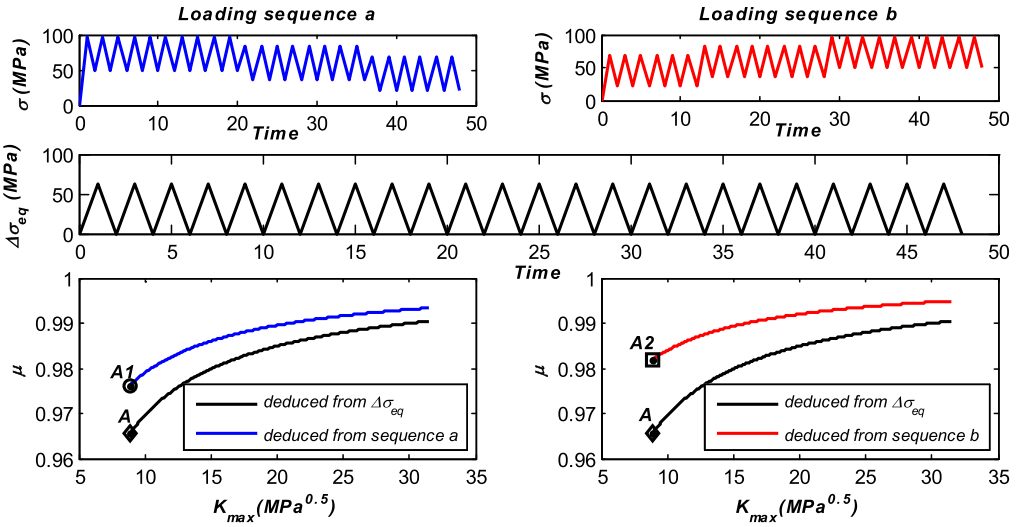

Figure 13. Variation of μ as a function of $K_{\max}$ for three loading sequences.

coefficient corresponding to point A2, where the residual stresses are based on the variable loads (loading sequence b).

This means that the loading sequence is not taken into account in the following calculation methodology.

5. Flowchart for determining the crack growth increment

The following flowchart illustrates the method for determining the fatigue cycle growth increment in relation to a fatigue crack growth increment (Figure 15).

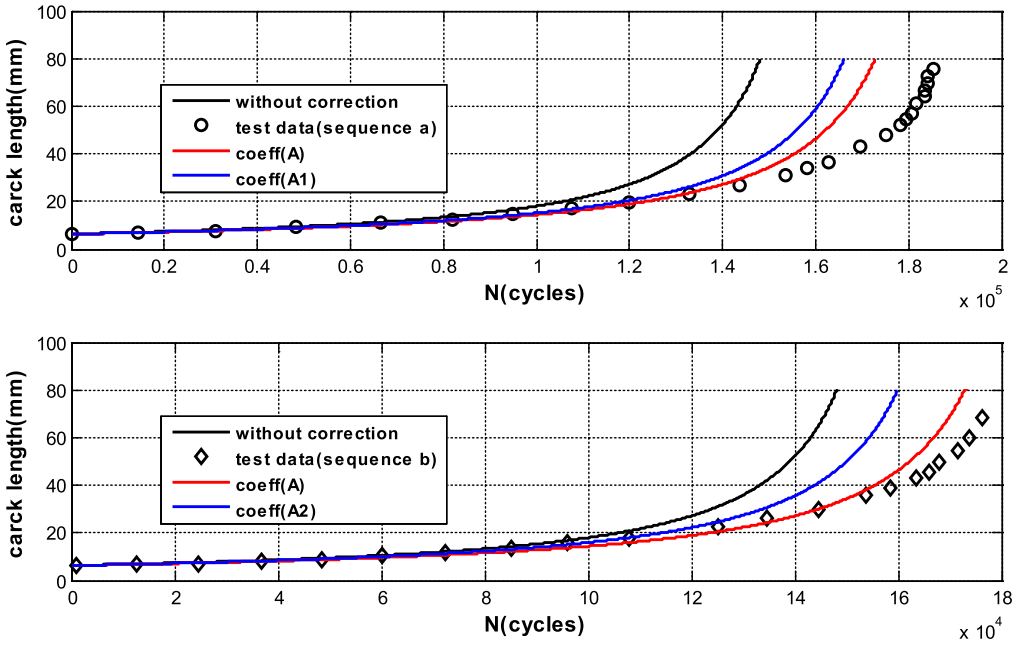

Figure 14. Effect of the correction coefficient on the evolution of the crack for different points.

6. Application of the model for different load sequences

To validate the computational model, three loading sequences are studied [30,33]. The first sequence is shown in (Figure 16a), where the maximum load is constant and equal to 83 MPa, with a variation of $\Delta\sigma$ from 75 MPa to 55 MPa and 14 MPa. The (Figure 16c) shows the second loading sequence (low-high) with three loading blocks, where the maximum stress is increased from 69 MPa to 83 MPa and then to 96 MPa, giving a constant $\Delta\sigma$ equal to 49 MPa. In (Figure 16e), we have a loading sequence of four loading blocks (top–bottom) with a constant $\Delta\sigma$ equal to 49 MPa.

For each loading sequence:

(i) The equivalent stress $\Delta\sigma_{eq}$ is calculated.
(ii) Using the Chaboche model, the residual stresses close to the crack are assessed.
(iii) The residual stress intensity factor is determined.
(iv) The correction coefficient is determined from which the corrected equivalent stress $\Delta\sigma_{eq\_corrected}$ is calculated.

We move from studying a variable cyclic charge spectrum problem to a constant charge spectrum problem.

Comparison of the results in Figure 16(b,d,f) shows that the experimental results are in agreement with the data from the fatigue life prediction model. Indeed, the crack propagation prediction curve reproduces, in most cases, the experimental data [30] than the one proposed by reference [17], who design and evaluate effective probabilistic methods allowing real-time prognosis of fatigue damage in structures, taking into account uncertainties related to loading, material properties and in situ diagnostics, based on the idea of finding an equivalent crack growth process under constant amplitude loading, which products a similar crack kinetics with that of the true random loading case. This constant amplitude loading is modified in this

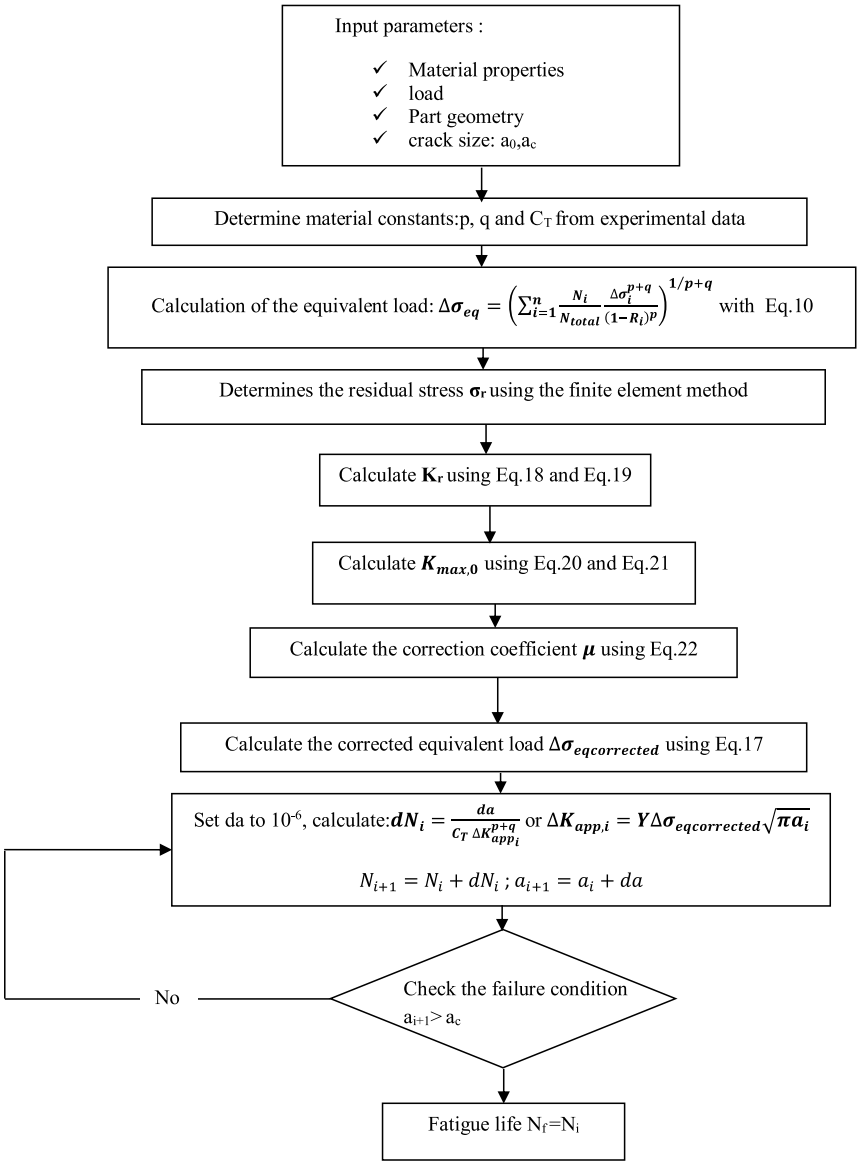

Figure 15. Flowchart for determining the crack growth increment.

section by integrating the effect of residual stress determined by the FE method and which are then introduced into the calculation of the equivalent loading. Corresponding to Figure 9, it is observed that the compressive stress distribution increases in absolute value near the crack tip, which is confirmed by the results of several researchers [32]. Since in our model, the evaluation of the applied equivalent stress is more reliable. A notable difference between the calculation model described in reference [17] and the experimental data occurs in the case of the second and third spectrum, which is corrected in our model by taking into account the effects of the residual stress determined by the FE method and which is then introduced into the calculation of the equivalent loading.

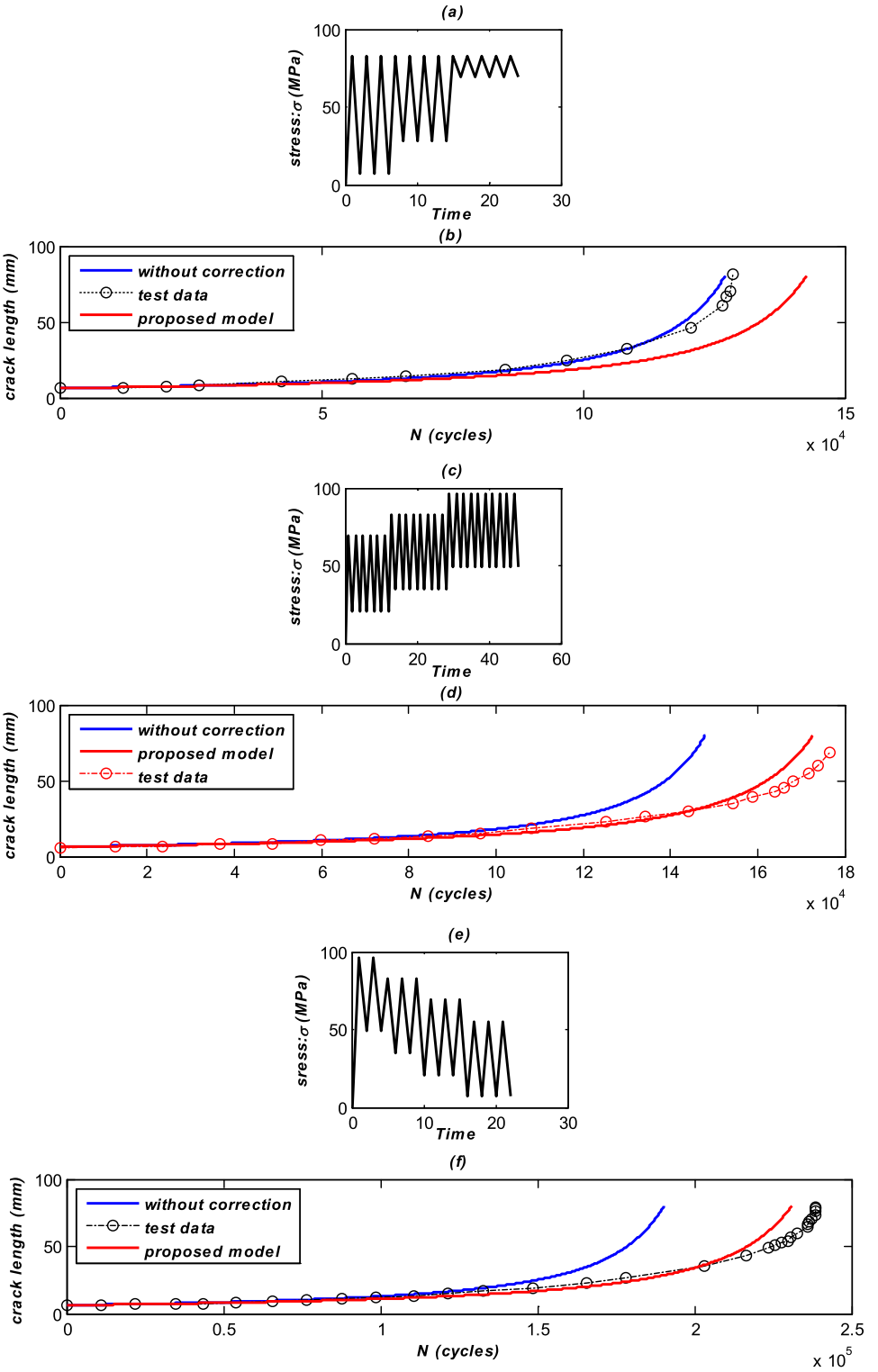

Figure 16. (b,d,f) Comparison of model results with experimental results for 2024-T3 aluminium [30] and model [17], using three types of variable loading spectra applied (a,c,e).

7. Conclusion

This study aims to provide a simple and effective approach to predicting fatigue life under variable loading by transforming variable load blocks into constant loads, thereby simplifying evaluation while preserving the essential mechanical effects. The influence of plastic deformations at the crack tip is accounted for with a correction coefficient that adjusts crack propagation predictions across different loading sequences. This correction improves agreement with experimental results. The following conclusions can be drawn:

(i) The stress-equivalent transformation approach avoids cycle-by-cycle calculations and reduces computational cost.
(ii) The correction coefficient has a stronger effect for low-to-high loading than for high-to-low, highlighting the importance of load order and loading dynamics on residual damage.
(iii) The model shows better agreement with experimental data when corrections due to plastic variations and residual damage are included, validating the usefulness of the proposed approach for diverse loading types.
(iv) Residual compressive stresses generally slow crack growth, but they exhibit substantial dispersion and large deformations; these aspects are incorporated into the model through the correction coefficient and the consideration of mean loading.

Nomenclature

$K_{\max}$	Maximum stress intensity factor
$K_{\max,i}$	Maximum stress intensity factor in the ith cycle
$K_{\max\_tot}$	Total maximum stress intensity factor
$K_{\max\_app}$	Maximum applied stress intensity factor
K_{r}	Residual stress intensity factor
ΔK	Stress intensity factor range
ΔK_i	Stress intensity factor range in the ith cycle
ΔK_{tot}	Total stress intensity factor range
ΔK_{app}	Applied stress intensity factor range
ΔK_{eff}	Effective stress intensity factor range
$\Delta\sigma$	Stress level
$\Delta\sigma_i$	Stress level in the ith cycle
$\Delta\sigma_{\mathrm{eq}}$	Equivalent stress level
$\Delta\sigma_{\mathrm{eq\_corrected}}$	Corrected equivalent stress level
a	Crack length
a_i	Crack length in the ith cycle
b	Width of specimen
a_0, a_{c}	Initial and critical crack lengths, respectively
Δa	Increment of crack length
Y	Geometric correction factor
R	Stress ratio
R_i	Stress ratio in the ith cycle
$\sigma_{\min}$ and $\sigma_{\max}$	Minimum and maximum stress, respectively
N_{tot}	Total number of loading cycles
N_i	Number of loading cycles in the ith cycle
C, C_T, p and q	Material parameters
μ	Correction coefficient
μ_i	Correction coefficient in the ith cycle
m	Weight function
P	Applied load

Declaration of interests

The authors do not work for, advise, own shares in, or receive funds from any organization that could benefit from this article, and have declared no affiliations other than their research organizations.

References

[1] E. R. Sérgio, F. V. Antunes and D. M. Neto, "Improving the fatigue crack growth prediction by accurate calibration of the constitutive material parameters", *Theoret. Appl. Fract. Mech.* **138** (2025), article no. 104957.

[2] A. H. Noroozi, G. Glinka and S. Lambert, "A study of the stress ratio effects on fatigue crack growth using the unified two-parameter fatigue crack growth driving force", *Int. J. Fatigue* **29** (2007), pp. 1616–1633.

[3] A. Remadi, A. Bahloul and C. H. Bouraoui, "Fatigue crack growth behavior of AA2024T3 under mixed mode loading within the framework of EPFM", *J. Mech. Sci. Technol.* **37** (2023), no. 4, pp. 1761–1771.

[4] O. E. Wheeler, "Spectrum loading and crack growth", *J. Basic Eng.* **94** (1972), pp. 181–186.

[5] F. Wang, J. Zheng, K. Liu, M. Tong and J. Zhou, "Numerical analysis of crack propagation in an aluminum alloy under random load spectra", *Modelling* **5** (2024), no. 2, pp. 424–437.

[6] W. Elber, "Fatigue crack closure under cyclic tension", *Eng. Fract. Mech.* **2** (1970), pp. 35–47.

[7] A. Garcia-Gonzalez, J. A. Aguilera, P. M. Cerezo, C. Castro-Egler and P. Lopez-Crespo, "A literature review of incorporating crack tip plasticity into fatigue crack growth models", *Materials* **16** (2023), no. 24, article no. 7603.

[8] G. Glinka and A. Buczynski, "Experimental and numerical analysis of elastic–plastic strains and stresses ahead of a growing fatigue crack", in *Workshop on Characterisation of Crack Tip Stress Fields* (L. Susmel et al., ed.), GruppoItalianaFrattura: Forni di Sopra, Italy, 2011.

[9] Q. Wu, Y. Zhao and X. Liu, "Fatigue life prediction of metal materials under random loads based on load spectrum extrapolation", *Int. J. Fatigue* **187** (2024), article no. 108473.

[10] A. H. Noroozi, G. Glinka and S. Lambert, "A study of the stress ratio effects on fatigue crack growth using the unified two-parameter fatigue crack growth driving force", *Int. J. Fatigue* **29** (2007), pp. 1616–1633.

[11] J. Willenborg, R. M. Engle and H. A. Wood, *A crack growth retardation model using an effective stress concept*, Technical Report, Wright Patterson Air Force Lab: Wright-Patterson AFB, OH, USA, no. AFFDL-TM-71-1-FBR, 1971.

[12] M. A. Meggiolaro and J. T. P. Castro, "Comparison of load interaction models in fatigue crack propagation", in *XVI Congresso Brasileiro de Eng. Mecânica (COBEM)*, ABCM: Uberlândia, MG, 2001, pp. 247–256.

[13] R. A. Neto, A. E. A. Chemin, W. W. Bose Filho and C. T. Ruchert, *On the use of NASGRO software to estimate fatigue life under constant and variable amplitude loadings in aluminum alloy SAE-AMS 7475-T7351*, 2023.

[14] P. Gallagher, *A generalized development of yield zone models*, Technical Report, Wright Patterson Air Force Lab: Wright-Patterson AFB, OH, USA, no. AFFDL-TM-74-28-FBR, 1974.

[15] G. Henauff and F. Morel, *Fatigue of Structures: Endurance, Design Criteria, Crack Propagation, Fracture*, Ellipses: Paris, 2005.

[16] S. Jiang, W. Zhang and Z. Wang, "Probabilistic fatigue crack growth analysis under stationary random loading with spike loads", *IEEE Access* **6** (2018), pp. 16878–16886.

[17] Y. Xiang and Y. Liu, "Efficient probabilistic methods for real-time fatigue damage prognosis", *Annu. Conf. PHM Soc.* **2** (2010), no. 1, pp. 1–12.

[18] T. L. Anderson, *Fatigue Crack Propagation Fracture Mechanics: Fundamental and Application*, 3rd edition, CRC Press: Boca Raton, FL, 2005, pp. 451–507.

[19] N. E. Dowling, M. V. Kral and S. L. Kampe, *Mechanical Behavior of Materials: Engineering Methods for Deformation, Fracture, and Fatigue*, 5th edition, Pearson Education, Inc.: Hoboken, NJ, 2019.

[20] A. J. McEvily, "Phenomenological and microstructural aspects of fatigue", in *Third International Conference on the Strength of Metals and Alloys, Cambridge, England*, The Institute and The Iron and Steel Institutes, Publication, W36, 1974, pp. 204–213.

[21] R. W. Lardner, "A dislocation model for fatigue crack growth in metals", *Philos. Mag.* **17** (1968), no. 145, pp. 71–82.

[22] T. Sireteanu, A. M. Mitu, M. Giuclea, O. Solomon and D. Stefanov, "Analytical method for fitting the rambergosgood model to given hysteresis loops", *Proc. Rom. Acad. Ser. A - Math. Phys. Tech. Sci. Inf. Sci.* **15** (2014), no. 1, pp. 35–42.

[23] A. Remadi, A. Bahloul and C. Bouraoui, "Residual plastic zone in front of crack tip under variable amplitude loading", in *International Conference Design and Modeling of Mechanical Systems*, Springer International Publishing: Cham, 2021.

[24] A. Remadi, A. Bahloul and C. Bouraoui, "Prediction of fatigue crack growth life under variable-amplitude loading using finite element analysis", *C. R. Mec.* **347** (2019), pp. 576–587.

[25] Dassault Systèmes Simulia, Inc. (DS Simulia Corp.), *ABAQUS/Standard User's Manual (Version 6.14)*, Dassault Systèmes Simulia, Inc. (DS Simulia Corp.), 2014/2015.

[26] P. Hu, Q. Meng, W. Hu, F. Shen, Z. Zhan and L. Sun, "A continuum damage mechanics approach coupled with an improved pit evolution model for the corrosion fatigue of aluminum alloy", *Corros. Sci.* **113** (2016), pp. 78–90.

[27] G. Glinka and G. Shen, "Universal features of weight functions for cracks in mode I", *Eng. Fract. Mech.* **40** (1991), no. 6, pp. 1135–1146.

[28] P. Kumar, *Elements of Fracture Mechanics*, McGraw-Hill Education LLC: New York, NY, 2009.

[29] Z. Lu and Y. Liu, "A comparative study between a small time scale model and the two driving force model for fatigue analysis", *Int. J. Fatigue* **42** (2012), pp. 57–70.

[30] S. Mikheevskiy and G. Glinka, "Elastic–plastic fatigue crack growth analysis under variable amplitude loading spectra", *Int. J. Fatigue* **31** (2009), no. 11–12, pp. 1828–1836.

[31] T. Kebir, B. Mohamed and M. Abdelkader, "Simulation of the cyclic hardening behavior of aluminum alloys simulation of the cyclic hardening behavior of aluminum alloys", *Mech. Eng.* **79** (2017), pp. 240–250.

[32] A. Bahloul and C. H. Bouraoui, "The overload effect on the crack tip cyclic plastic deformation response in SA333 Gr 6 C-Mn steel", *Theoret. Appl. Fract. Mech.* **99** (2018), pp. 27–35.

[33] W. J. Wang and M.-S. Yim, "A fatigue crack growth prediction model for cracked specimen under variable amplitude loading", *Int. J. Fatigue* **168** (2023), article no. 107387.